J. Earth Syst. Sci. (2020)129 87
https://doi.org/10.1007/s12040-020-1357-5

Soft-sediment deformation structures in a Permo-carboniferous glacio-marine setting, Talchir Formation, Dudhi Nala, India

H N Bhattacharya* and Amrita Mukherjee

Department of Earth Sciences, Techno India University, Sector-V, Salt Lake, Kolkata, India.
**Corresponding author. e-mail: hbaruamu@gmail.com*

MS received 7 October 2019; revised 19 December 2019; accepted 26 December 2019

The Permo-carboniferous glacio-marine Talchir Formation of Dudhi Nala, West Bokaro Coal Basin, India, hosts soft-sediment deformation structures that originated from liquefaction and concomitant fluidization of unconsolidated sediments at or close to the sediment–water interface. Since liquefaction of water saturated sediments may be initiated by different endogenic or exogenic triggering agents, identification of the trigger needs careful analysis of the deformation structure, as well as depositional mechanism and environment of deposition of the host sediments. In-depth analysis of the studied liquefaction- and fluidization-induced soft-sediment deformation structures and sedimentary attributes of the host sediments of the studied succession unequivocally stand against the role of strong wave and tidal action, rapid sediment loading, mass-flow and subaqueous slides related shear stress, and water or gas seepage as the triggering agent. However, development of the soft-sediment deformation structures, close to sediment–water interface, closeness to syn-sedimentary fault, flowage along the tilt towards the fault, confinement within undeformed beds, episodic character and close similarities with structures that are formed during recent earthquakes, are consistent with seismic triggering for liquefaction. The studied shallow marine sediments record a sequel of climatic amelioration, glacial retreat, shallow marine sedimentation, glacio-isostatic rebound and related syn-sedimentary faulting and development of soft-sediment deformation structures.

Keywords. Sedimentary; soft-sediment deformation structures; seismite; Talchir Formation; Gondwana Supergroup.

1. Introduction

Soft-sediment deformation structures (hereafter referred to as SSDS) are formed after sedimentation but before lithification (Allen 1984), and some of them provide clues to contemporary basin dynamics (Seth *et al.* 1990; Bhattacharya and Bandyopadhyay 1998; Davies and Gibling 2003; Campbell *et al.* 2006; Chen *et al.* 2009; Van Loon 2009; Owen and Moretti 2011). Finer siliciclastic heterolithic sediments and carbonate successions of shallow marine and lacustrine environments are the main repositories of such SSDS (Mastalerz and Wojewoda 1993; Owen 1996; Bhattacharya and Bandyopadhyay 1998; Sarkar *et al.* 2014), and liquefaction and concomitant fluidization are held responsible, in majority of cases, for their origin (Ten Haaf 1956; Allen 1975, 1984; Chakraborty 1977; Owen 1996; Moretti *et al.* 1999; Owen and Moretti 2011). Syn-sedimentary seismic activity is

Published online: 04 March 2020

held as the main triggering agent for liquefaction and concomitant fluidization (Seilacher 1969; Sims 1973, 1975; Lowe 1975; Allen 1986; Seth *et al.* 1990; Ghosh 1993; Bhattacharya and Bandyopadhyay 1998; Zhang *et al.* 2007; Su and Sun 2012; Zheng *et al.* 2015; Snyder and Waldron 2016; Jiang *et al.* 2016; Lunina and Gladkov 2016; Onorato *et al.* 2016; Toro and Pratt 2016 and many others cited in Shanmugam 2016). However, similar structures may form by pounding waves (Alfaro *et al.* 2002), meteorite impact (Alvarez *et al.* 1998), subaqueous mass movement (Owen and Moretti 2008), shear stress along sediment water interface (Greb and Archer 2007), rapid sedimentation (Lowe 1975; Postma 1983), overloading (Moretti and Sabato 2007; Owen and Moretti 2008; Chiarella *et al.* 2016) and ground water/gas movement (Massari *et al.* 2001; Hilbert-Wolf *et al.* 2016). Hence, to resolve the controversy, soft-sediment deformation structures should be analysed in the frame of all other available geological information, a context-based approach of Owen and Moretti (2011), for the best diagnostic results, since all triggering agents keep some finger prints as depositional or erosional evidences.

The Talchir Formation of Dudhi Nala (a rivulet), Hazaribagh, India, a Permo-carboniferous glacio-marine sedimentary succession (Bhattacharya *et al.* 1989; Bose *et al.* 1992; Mukhopadhyay and Bhattacharya 1994) contains well developed SSDS. Absence of post-depositional deformations, predictable facies control and occurrences close to syn-sedimentary faults offer unique opportunities to track the stages of evolution of SSDS along with their triggering agents in a more comprehensive way. The present contribution aims to constrain the evolution of such SSDS developed in Talchir sediments of Dudhi Nala with their possible triggering agent/s.

2. Geological setting

The Gondwana Supergroup (Late Carboniferous to Early Cretaceous) represents the most important coal-bearing sedimentary succession of Indian subcontinent (Mukhopadhyay *et al.* 2010). The sediments of Gondwana Supergroup (table 1) occur in isolated basins within regionally developed intracratonic rift system in Indian subcontinent (figure 1). Initial sedimentation took place under glacio-marine setting, represented by Talchir Formation (Late Carboniferous to Early Permian), which is followed upward by coal-bearing fluviatile sediments of younger Formations (Bhattacharya *et al.* 2005). Well preserved and continuous exposures of Talchir Formation are available along the course of the Dudhi Nala in West Bokaro coal basin (figure 1). In other parts of the basin, the sediments of Talchir Formation are covered by thick soil. The glacio-marine sediments of the Talchir Formation (Bhattacharya *et al.* 1989; Bose *et al.* 1992; Mukhopadhyay and Bhattacharya 1994; Bhattacharya *et al.* 2005) unconformably overlie Precambrian basement of granitoid and amphibolite rocks (figure 1). Altogether three facies

Table 1. *A generalized stratigraphy of the Gondwana Supergroup of Indian subcontinent.*

Supergroup	Group	Formation	Age
	Post Gondwana	Bagh bed–Lameta bed–Deccan Traps	Upper Cretaceous
Gondwana	Upper Gondwana	Umia–Uttattur Formation	Late Lower Cretaceous
Supergroup	Group	Rajmahal–Jabalpur Formation	Early Lower Cretaceous
		Chilika–Gangapur Formation	Upper Jurassic
		———*Middle Jarassic break*———	
		Kota Formation	Lower Jurassic
		Mahadeva–Pachmarhi–Maleri–Tiki Formation	Upper Triassic
		Yerapalli Formation	Late Lower Triassic
		Panchet–Persora–Mangli Formation	Early Lower Triassic
		———*Permo-Triassic break*———	
	Lower Gondwana	Raniganj–Pali Formation	Late Upper Permian
	Group	Barren Measure–Ironstone Shale Formation	Early Upper Permian
		Barakar Formation	Late Lower Permian
		Karharbari Formation	Early Lower Permian
		Talchir Formation	Upper Carboniferous to Early Lower Permian

Basement: composed of Precambrian granitoids and metamorphics along with Proterozoics sediments.

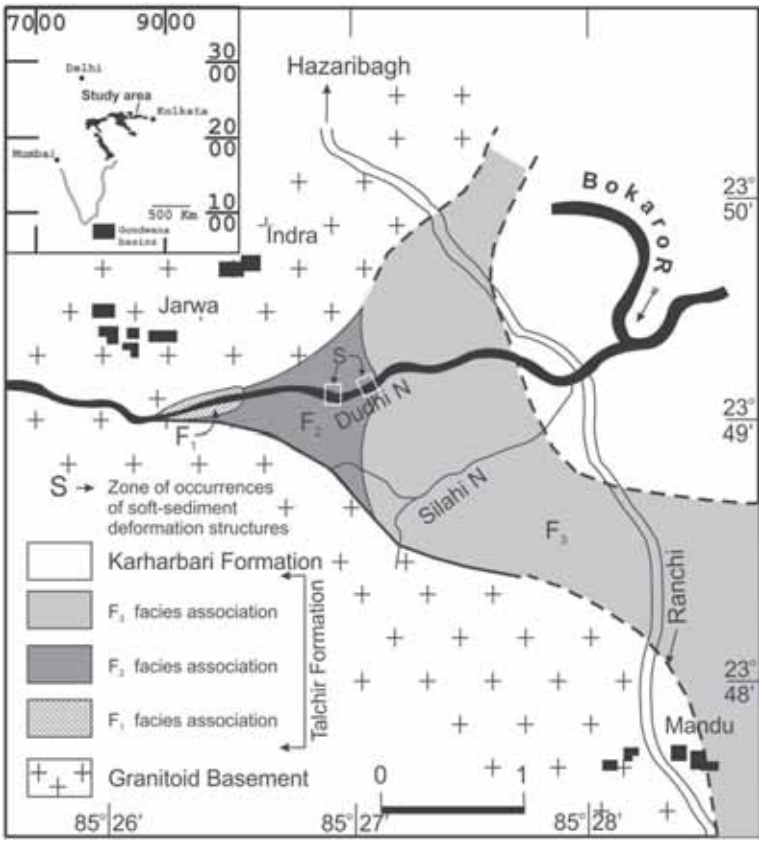

Figure 1. Geological map of Talchir Formation, exposed in Dudhi Nala section of West Bokaro Coal Basin (modified after Bhattacharya *et al.* 2005), showing distribution of different facies association and locality of seismite occurrences (marked S). The map in the inset showing the rift-bounded Gondwana basins in the Indian subcontinent and the study area.

associations with distinguishable facies types constitute the Talchir Formation of West Bokaro coal basin (figure 1 and table 2). The basal facies association F1 is dominated by conglomerates of glaciogenic and reworked glaciogenic origin deposited in a fjord like, easterly opening trough on basement rocks (Bose *et al* 1992; Mukhopadhyay and Bhattacharya 1994). The basal conglomeratic F1 facies association is overlain by a ∼38 m thick facies association F2 of plane-laminated well-sorted sandstone facies, thinly laminated sandstone-muddy siltstone facies, hummocky cross-stratified sandstone facies, conglomerate facies and channel-fill fine sandstone facies representing ice-marginal shore face environment (Mukhopadhyay and Bhattacharya 1994). The basal shore face plane-laminated well sorted sandstone facies of F2 facies association onlapped all the sediments of the F1 facies association at a low angle (10°–15°). The abrupt transgression might be a consequence of progressive deglaciation and climatic amelioration (Bhattacharya *et al* 1989). The F2 facies association is again overlain by F3 facies association containing dropstone free sandstone–mudstone heteroliths of deeper slope environment. The change over from shore face to outer slope environment is abrupt and the heteroliths of F3 facies association overlies hummocky cross-stratified sandstone facies of F3 facies association. The dropstone free sandstone–mudstone heteroliths represent a phase of total deglaciation and further deepening of the basin. Glacio-isostasy might have played an important role behind such foundering of the Talchir basin (Bhattacharya *et al.* 2005). Sengupta *et al.* (1999) reported marine fossil *Polyplacophora* from this succession. The fining and thinning upward glacio-marine Talchir succession had been deformed by the development of horst-graben structures under the influence of isostatic crustal rebound after the removal of thick ice cover (Bhattacharya *et al.* 2005). Such an ice house to greenhouse climatic change influenced continental to shallow marine sedimentation of sandstone–shale–coal of younger Gondwana Formations along such grabens (Bhattacharya *et al.* 2005).

Table 2. *Facies association and facies types of Talchir Formation of Dudhi Nala with their descriptions and interpretations.*

	Facies type	Facies description	Interpretation
Facies association F1	*In-situ* breccias	Occur as a skin over the bedrock at the upper reaches of the trough, exhibits polygonal blocks of granite and amphibole with matching boundaries, the narrow interstitial spaces filled with pebbly siltstone	Formed after intense fracturing of bedrock due to repeated freezing of percolating water during glacial phase
	Jagged breccias	Jagged mass of crudely parallel, elongate granite and amphibolite blocks without matching boundaries. Gaps between blocks are filled up with pebbly and muddy sandstone	Result of down slope creep and slump of materials of *in-situ* breccias
	Tabular clast supported conglomerate	Stacked tabular granite boulders with their upper surface faceted, striated and well-polished, representing lodgement tillite	The stacking of the boulders and sheared fines between them are attributed to selective sub-glacial lodgement
	Silty sandstone	This facies observed near the western margin of Talchir outcrop area, represents silty sand bodies filling sub-horizontal fractures within solid granite basement	This facies are formed presumably under pressure of sloughing ice mass indicates glacial environment
	Pebbly–sandstone/siltstone alternations	Alternations of normally graded buff-coloured fine to medium-grained sand and massive or faintly plane-laminated green silt	Reworked product of subglacial, englacial and superglacial materials through various types of sediment gravity flows
	Reverse graded conglomerate – sandstone alternations	Wedge-shaped beds of inversely graded pebbly conglomerates alternating with laterally persistent commonly massive and locally plane-laminated fine sandstones	Subglacial sediment gravity flow deposit Massive sandstone beds deposited from turbidity currents emerging from the gravel-depositing denser underflows
	Chaotic angular matrix supported conglomerate	Chaotic matrix-supported conglomerate with angular, large-sized faceted and striated clasts	Subglacial sediment gravity flow deposit
	Chaotic, rounded, matrix-supported conglomerate	Chaotic matrix-supported conglomerate, with constituent clasts having a high degree of roundness and sphericity. Many clasts are, faceted	Subglacial sediment gravity flow deposits with clasts inherited from earlier deposits
Facies association F2	Plane laminated well-sorted sandstone	Sandstone with millimetre-thick plane lamination, well sorted and mud-free	Beach face sand, possibly on the upper shoreface
	Thinly laminated sandstone–muddy siltstone alternations	Green silt sometimes grading into mud alternates repetitively with millimetre to centimetre thick sandstones with plane lamination, bi-directional ripple cross-laminations, climbing ripple cross-laminations and combined flow ripple cross-laminations	Tidal bundles in upper shore face embayments
	Hummocky cross-stratified sandstone	Well-sorted hummocky cross-stratified sandstone dra pes erosional plane on graded sand-silt alternation faces. This sandstone is free of dropstones	Storm laid sand deposited on shore face

Table 2. *(Continued.)*

	Facies type	Facies description	Interpretation
	Conglomerates	Conglomerates with (1) matrix-supported disorganised fabric, (2) clast-supported with reverse grading and locally, (3) clast-supported with normal grading dominate the upper part of the facies architecture of this facies association. Shear planes or scouring are common along the basal	Various types of sediments gravity flow deposits along rip-current and/or storm surge channels with clasts derived from in trough F1 facies association. Preponderance of such coarser deposits in the upper part of the succession indicates down sagging of the basin floor that ushered in coarser mass-flows, possibly along rip-current or storm-surge channels
	Channel-fill fine sandstone	Superposed channels filled up with plane to ripple bedded fine sandstone. In the lower part of the facies architecture the channel-fill sediments are confined within channels and in the middle and upper part the channel-fill sediments spill over the channel banks	Subaerial to subaqueous channels filled up with shore face sediments. The channels are produced by basin ward storm surges and later filled up with shore face sediments
Facies association F3	Thin-bedded fine sandstone –siltstone– mudstone alternation	Laterally persistent millimetre to centimetre thick fine grained sand, silt and mud alternation characterise this facies, whose aggregate thickness may vary from 2 to 167 cm. Sands are often normally graded or parallel and ripple cross-laminated. Grooves and flutes are common on soles	Low-density turbidites deposited below storm weather wave base. Some units may represent storm surges below storm weather wave base
	Thin and massive sandstone with floating mudstone clasts	Millimetre to centimetre thick parallel sided massive sandstones with floating mud clasts near the bed top. Shear planes are common near the base. Sandstone beds are encased within mudstones	Debrites in mud depositing outer fan
	Thick multi-storied sandstones	Wide but lenticular sharp based, amalgamated sandstone bodies, thickness varying between 15 and 200 cm, often grade into mudstone. Massive to normally graded near the base and plain to ripple cross-laminated near top. The top of the sand beds are sometimes bioturbated	Channel-fill turbidites in mid- to outer-fan segments

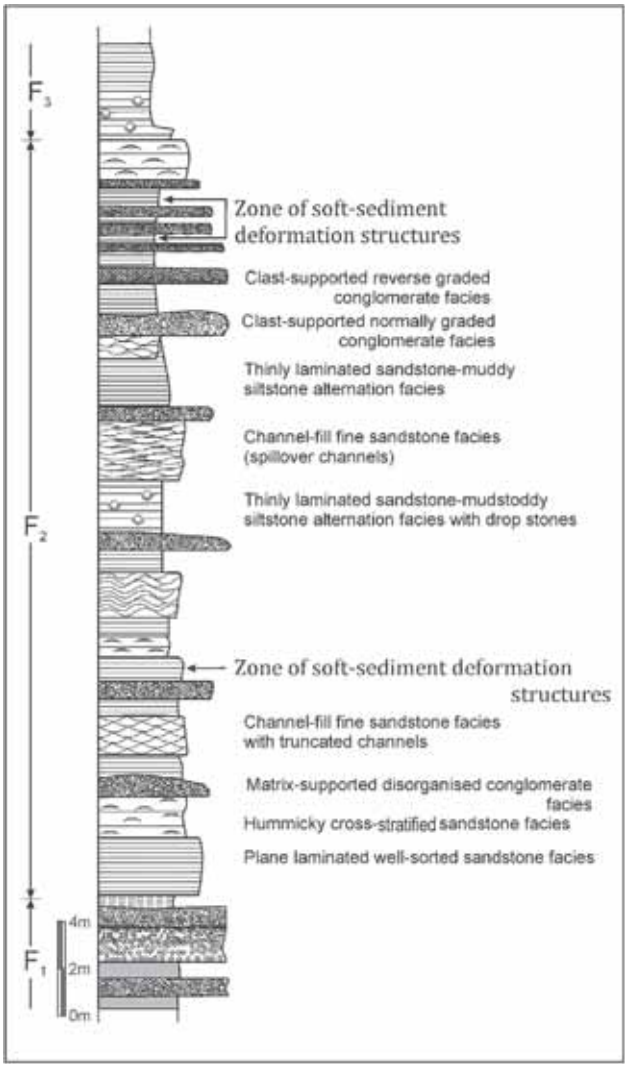

Figure 2. Architecture of facies types of sandstone–siltstone facies association (F2) of Talchir Formation, in Dudhi Nala section.

3. Soft-sediment deformation structures

SSDS are developed in graded sandstone–siltstone facies sediments and are common near the central and upper parts of the facies architecture of F2 facies association. Though SSDS occurs at three different stratigraphic levels (figure 2), they are temporally restricted in short stratigraphic intervals of <1 m thick. Moreover, they also occur close to a major intrabasinal sub-vertical normal fault (figure 3a). Innumerable minor sub-vertical synsedimentary faults (figure 3b), with variable throw across the fault plane are developed in the close vicinity of this major fault, suggesting intermittent movements along the major fault during sedimentation. However, restricted exposure of Talchir sediments along the course of Dudhi Nala does not allow outcrop study to judge the spatial continuity of SSDS bearing horizons for longer stretches. Detailed description and possible genetic interpretation of the SSDS present in Talchir Formation of Dudhi Nala is given below.

3.1 *Graben-like down sagging structure*

Graben-like down sagging structure is developed in flat bedded and graded sandstone–siltstone facies (figure 4a). Sagging along two sets of normal faults, facing each other, creates the Graben-like structure. The oppositely dipping normal faults are of listric type and show maximum separations near the base. There are numerous smaller normal faults developed within the graben-like structure, with decreasing throw towards top (figure 4a). The underlying muddy siltstone layer is thinner below the graben and thicker on either sides beyond the graben (figure 4a). Undeformed thin (2–4 cm) and horizontal sandstone–siltstone alternations overlie the graben-like down sagging structure. This structure is developed within 6 m from a major intrabasinal fault. Other soft-sediment deformation structures, such as torn beds and slump folds (discussed later), are developed close to this structure.

An identical structure has been described by Sims (1975, figure 2) from Van Norman Lake sediments, which was formed during the July 21, 1952 Kern Country, California earthquake. Similar structures are common in seismites of the Paleoproterozoic Chaibasa Formation of Dhalbhumgarh and Ghatsila, India (Bhattacharya and Bandyopadhyay 1998) and have also been reported from alluvial fans developed in an active strike-slip fault setting (Plio–Pleistocene) from south-western Poland by Mastalerz and Wojewoda (1993). Seth *et al.* (1990) also described similar structures of probable seismic origin from the Late Jurassic Katrol Formation of Kutch (India) and considered earthquake as a triggering agent. Van Loon (2009), however, suggested that similar structures may originate from melting of buried ice below the graben structure.

Ghosh (1993), from test model experiments, suggested horizontal extension of the floor with very low shear strength had been responsible for the development of such graben-like structures. Horizontal extension of a sediment layer may occur in a liquefied state. The influence of cyclic and/or

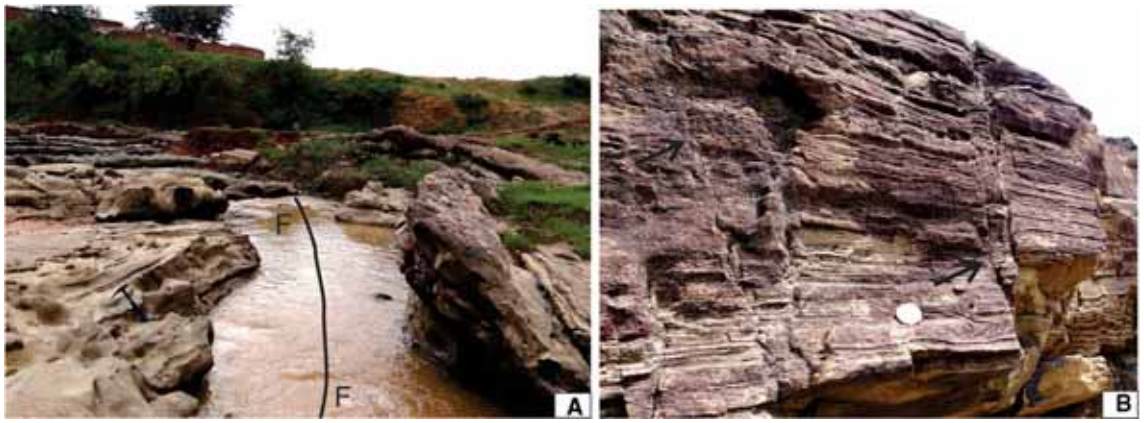

Figure 3. (**a**) Field photographs of a major intrabasinal faults (arrow marked) developed close to the occurrences of SSDS. (**b**) Syn-sedimentary parasitic faults developed in the close vicinity of the major intrabasinal fault, shown in figure (a).

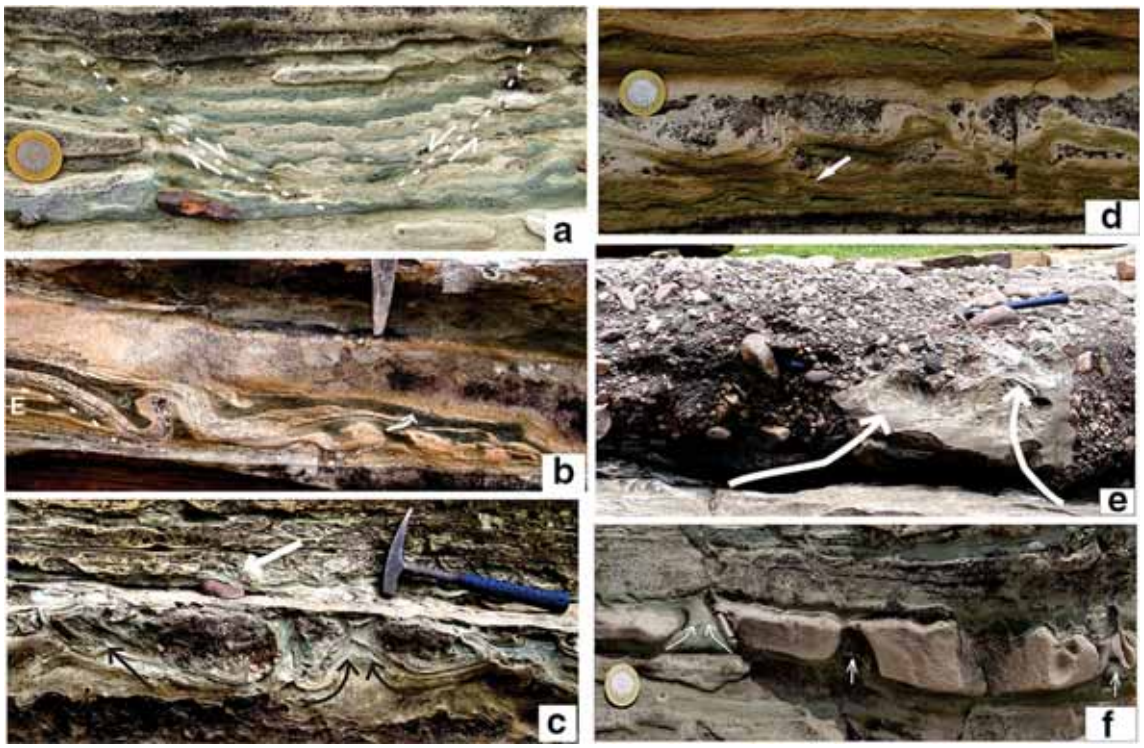

Figure 4. Field photographs of the studied SSDS of Dudhi Nala section. (**a**) Graben-like down sagging structure is developed in graded sandstone–siltstone–mudstone facies. Movement directions on oppositely dipping faults are shown. Note the reduced thickness of the siltstone layer below the graben; (**b**) slump folds in graded sandstone–muddy siltstone facies. Note the slump beds are rolled and torn apart with flowage of fluidized mud along the gaps (arrow marked), away from the scour surface (marked E); (**c**) convolute laminations in graded sandstone–muddy siltstone facies, with broad troughs and sharp crests. Note siltstone draping over the erosional top of the convolute laminations and strewn ice rafted debris (white arrow marked); (**d**) load structures, note the asymmetricity of the load structures and development of shear folds (arrow marked) near the base; (**e**) piercing muddy siltstone dykes in conglomerate (arrow marked), note the churned contact between the two facies; and (**f**) ruptured beds, inverted V shaped gaps in sandstone are filled up with fluidized muddy siltstone (arrow marked). Note the degree of rupturing increases from left to right of the exposure.

incremental loading on pore water in water saturated sediments results in liquefaction and total loss of shear resistance. Apart from seismic shocks, pounding waves, meteorite impact, shear stress related to tide or sub-aqueous mass movement, overloading due to rapid sedimentation may cause liquefaction of water saturated sediments. However, it is pertinent to note here that the graben-like down sagging structure is floored by a liquefied muddy siltstone layer, which is thinner below the

graben and recorded layer parallel flowage. Such intra-layer flow might have imposed extension in the immediately overlying soft but unliquefied heterolithic sediments that yielded in a normal fault controlled graben-like structure. Hence, the development of the graben-like down sagging structure is the manifestation of liquefaction of the underlying silt layer. Moreover, the graben is overlain and underlain by lithologically similar, but undeformed beds indicating a sudden change in conditions that lasted for a particular span of time for the deformation to take place. The presence of an undeformed and laterally persistent sandstone bed below the muddy siltstone bed, showing no evidence of liquefaction (figure 4a), negates the origin of these soft-sediment deformation structures from ground water upsurge or melting of underlying buried ice. At the same time, absence of any wave generated structure bearing sediments above negates the role of pounding waves for liquefaction. Moreover, mass-flow related shear planes are also absent in the overlying beds. The thinness of the beds of sandstone–siltstone alternations above the graben-like structure also stands against the possibility of increased sediment loading. However, closeness to syn-sedimentary fault and confinement in a particular stratigraphic horizon strongly advocates in favour of a sudden and time bound trigger, very similar to earthquake shocks, for the liquefaction of the siltstone layer below the graben-like down sagging structure. Decrease in rate of throw along the faults towards the top of the graben-like structure, suggests temporal waning of the rate of down sagging related to lateral stretching of the liquefied layer below the graben.

3.2 *Slump folds*

In the graded sandstone–siltstone alternation facies, two couplets of sand–silt alternations show evidence of sliding down along a low angle ($< 5°$) scour surface, developing slump folds (figure 4b). The slumped layers became thicker and developed disharmonic folds with unequal limbs and variably oriented axial planes. The slump beds are rolled and torn apart with evidence of fluidization as the silty sediments get teared and pierce through the sandstone layers (arrow marked in figure 4b). Both the contact of the slumped unit is erosional. Graded and undeformed sandstone (4 cm thick) occurs above the slumped unit. This soft-sediment deformation structure developed very close to a major fault (figure 3b) and occurs in the foot-wall block, which shows nearly 10° tilt towards the fault. Further, it is pertinent to note that the direction of slumping is towards the fault.

The smoothness of the folds with thickness change of the sandstone layers and ultimate rolling and tearing of sandy layers clearly point to their very low shear strength during slumping. Moreover, slumping along a horizontal to very low angle surface indicates flowage of a liquefied sediment having very low shear strength. Continuity of the slumped sandstone layers with occasional tearing possibly suggest that the silt layers were more liquefied than the sand layers and the higher liquefaction of silt gave the mobility for the lateral flowage. Upward flowage of silty sediments also facilitates fluid release at the later stage of liquefaction to bring about fluidization. Such a continuous process of liquefaction and related loss of shear strength, flowage and fluidization might have been triggered by an increase of pore fluid pressure due to cyclic loading related to vibratory ground motion of earthquake waves. This interpretation also gains support from the closeness to a syn-sedimentary fault. Moreover, the signatures of overloading, pounding waves, shear stress along bedding surface related to denser mass-flow or strong currents for liquefaction are absent.

3.3 *Convolute laminations*

Convolute laminations in graded sandstone–siltstone facies are with broad troughs in between mushroom-shaped antiformal crests (figure 4c). In one case, an upper unsorted, coarse and pebbly sandstone bed involved in convolution became detached and occurs as isolated kidney shaped bodies in the core of the troughs. The top part of the convolutions is truncated by an erosional surface, suggesting their metadepositional character (see Nagtegaal 1963). The erosional surface is draped by a thin ($\sim$1 cm) siltstone layer. A few ice rafted debris (IRD), drop stones, occur on this thin siltstone layer (marked in the figure). The laminations gradually become undeformed and flat near the base. The crests in between troughs are occupied by fine sandstone–siltstone intercalations with vertical, tightly folded laminations, which are pierced locally by fluid-escape channels. The folds on laminations in thin sandstone–siltstone couplets are very smooth and show variations in thickness of

the deformed layers from below the trough to the fluid-escape channels. There are three horizons containing convolute laminations, separated by undeformed beds. Such convolute structures are developed close to a syn-sedimentary fault.

Smoothness and extreme thickness variation of sandy and silty layers around a coarse sandstone core indicates very low shear strength of the sand-silt layers, involved in convolution due to liquefaction (see Allen 1977). The presence of coarse pebbly sandstone at the top of the convoluted layers imposed a strong unstable density gradient that might have enhanced the deformation mechanism. Development of convolute laminations along certain stratigraphic levels separated by undeformed beds indicates that the required conditions for liquefaction and concomitant fluidization developed episodically. Further, the occurrence of the convolute laminations below an undeformed erosional surface indicates that the deformation took place at the sediment–water interface and there was no sediment load above to trigger liquefaction. Fluidized silt, after piercing the laminations near the crests, was redistributed over the substrate to form a centimetre thick siltstone layer that drapes the erosional surface above the convolutes (also see Moretti *et al.* 1999). Mukhopadhyay and Bhattacharya (1994) interpreted the upper pebbly sandstone layer involved in convolution as fall-out sediments from floating ice-sheets undergoing melting. In this context, the presence of melt out sediments and drop stones in the siltstone layer above the convolutes indicates the presence of floating ice sheets in the shallower part of the sea, which dampens larger storm waves that may create liquefaction in the sediments near the sediment water interface. The absence of deformed beds below also indicates that upsurge of ground water was not responsible for the soft-sediment deformation. Hence, the episodic development, metadepositional nature and closeness to intrabasinal major and syn-sedimentary minor fault strongly suggests that earthquake waves acted as the triggering agent for liquefaction of alternating sand–silt sediments to form the studied convolute laminations. Further, development of three separate convoluted horizons also indicates repeated earthquakes.

3.4 *Load cast*

Load casts are formed along the base of a sandstone bed in sandstone–muddy siltstone alternations facies (figure 4d). This soft-sediment deformation structure is also located close to a major intrabasinal fault and the beds show low angle tilt towards the fault in an otherwise undeformed succession. The bottom contact of the sandstone with a muddy siltstone is characterised by broad synforms and sharp antiforms whereas the upper contact with muddy siltstone has remained straight and undeformed. The sandstones in the sandstone–siltstone heteroliths above the deformed beds are wave rippled. The antiforms in between loads are pierced by water escape channels or pillars. However, the pillars never crossed the sandstone layer entirely. The synformal loads are asymmetrical, with axial planes dipping in the same direction. The underlying thinly laminated heterolith is passively folded following the load casts in sandstone. Near the base of the deformed heterolith, the contact with the underlying sandstone is sheared with development of small asymmetric shear folds with long and short limbs. Alignments of the axial planes of the shear folds are identical with the axial planes of the load casts above. The sandstone lying below the deformed heteroliths is undeformed with flat top surface.

Liquefaction and concomitant fluidization of the lower part of the fine sandstone–muddy siltstone alternations caused sinking lobes of water saturated unlithified sands with water escape channels forming pillars in between. Liquefaction of the heterolithic sediments resulted in loss of shear resistance and a high density gradient between overlying sand and underlying finer sandstone–muddy siltstone leading to the formation of large load casts (see Moretti *et al.* 1999). Passive folding of the thinly laminated sand–muddy siltstone alternations around the load casts attests their very low shear strength. Further, the undeformed character of the upper part of the load casted sandstone layer possibly indicates that the lower half of the sandy sediment was more water saturated than the upper part. In the absence of compressive stresses in the studied basin, development of shear folds and related shear planes along the contact with underlying sandstone advocates in favour of flowage of the liquefied sediments on a low angle slope. Such flowage of a liquefied body of heterolithic sediments with decreasing degree of liquefaction upward resulted in simple shear related deformation along the contact with rigid sand below. The attitude of the asymmetrical folds and load structures also

indicates that the flowage took place towards the intrabasinal fault.

The observable sedimentary attributes in favour of large pounding waves, strong currents, high-density flows above the deformed beds, overlying sediment weight after quick sedimentation and groundwater upsurge as a trigger for liquefaction are absent in the studied section. In absence of sedimentary attributes of the aforesaid triggering processes, the present authors consider earthquake waves might have triggered the liquefaction required for the studied soft-sediment deformation structures. Further, development of the structure in close proximity to a major intrabasinal fault and flowage of the liquefied sediments following the tilt of the faulted block lend strong support for their genetic linkage with earthquake.

3.5 *Piercing siltstone dykes in conglomerate*

There are several reverse graded and normally graded conglomerates, formed by high-density sediment gravity flows along rip-current channels on shoreface, near the top of the F2 facies association architecture. However, in one such horizon the contact between a graded sandstone-muddy siltstone heterolithic facies and overlying reverse graded conglomerate facies is severely deformed and muddy siltstone dykes pierce through inter-gravel spaces in the conglomerate (figure 4e). A few large clasts have sunk well within the underlying deformed sandstone–siltstone heterolith.

Such piercing siltstone dykes through overlying thick sediments with high gravitational instability could have been generated by liquefaction and concomitant fluidization of finer sediments lying below. In the studied structure, the load of overlying thick conglomeratic sediments or shear stress, along the contact between high density mass-flow and underlying finer water saturated heterolithic sediment were competent enough to trigger liquefaction of the low density layers. But interestingly, such structure is developed involving only one conglomerate horizon, though there are number of similar conglomerate horizons that overlie finer sediments with well developed close-spaced shear planes, indicating strong basal shearing. In this context, vibratory ground motions as triggering agent gain support when similar structures in other conglomerates having evidence of basal shearing effects remain absent and development of such structures close to syn-sedimentary faults. However, role of shear stress near the base of the high density mass flow for such deformation cannot be ruled out.

3.6 *Ruptured beds*

A sandstone bed with a flat base and rippled top is ruptured (figure 4f). Such stretching of the sand bed produced blocks with decreasing size and increasing gaps in between from right to the left end of the exposure (see figure 4f). Where the gaps along fractures are partly developed, they are inverted V-shaped, closing towards top. The gaps between the sand blocks are filled up with muddy siltstone from below. Sediments lying below and above the deformed sandstone–muddy siltstone beds remained undeformed. Similar deformation recurred again after the deposition of 15 cm of undeformed sandstone–siltstone heterolithic facies beds.

This structure is interpreted as a product of layer parallel extension of the sand layer caused by lateral flowage of the liquefied muddy silt layer below. Inverted 'V' shaped gaps extended from base to the top of the torn sandstone bed allowed fluidization of muddy silt. Further, this also suggests that the rate of extension was much higher along the basal contact of the sand layer with the liquefied sediments than its upper part. The presence of undeformed sandstone–siltstone facies layers above the deformed beds indicates the rupturing took place at the sediment–water interface. In the absence of clues in favour of other triggering agents, an earthquake is considered the likely triggering agent for liquefaction and later fluidization of the muddy siltstone. The occurrence of the deformation structure within a distance of 5 m from a syn-sedimentary fault lends strong support to this contention.

4. Discussion

Owen and Moretti (2008) and Shanmugam (2016) have rightly pointed out that since earthquakes do not represent the deformation mechanisms in the formation of SSDS, coinage of the term 'seismite' without in depth analysis of each structure and its host succession may be misleading. The interpretation of triggering agent becomes complex because liquefaction and related fluidization, responsible for the development of the majority of such structures, could be conceivably triggered by several endogenic and exogenic agents (see Toro and Pratt 2016). Moreover, the morphology of these

structures does not depend on the triggering agent (Owen and Moretti 2011). Because of these complications, the identification of trigger or triggers for liquefaction of soft-sediments becomes more difficult. Most of the possible triggering agents for liquefaction of soft-sediments retain some unmistakable fingerprints in the form of unique sedimentary facies or sedimentary structures, but an earthquake trigger fails to emboss any direct and distinguishable evidence in the host sediments. To ease this difficulty, Owen and Moretti (2011) put forward some determining criteria for earthquakes as triggers for soft-sediment deformation due to liquefaction, such as large spatial continuity, vertical repetition, proximity to faults, matching structures that are formed during recent earthquake and zonation of complexity with distance from the fault. However, all these criteria may be fulfilled by one or other triggering agents as well (mentioned before), because all of them are equally efficient to liquefy a unconsolidated water saturated sediment and the situation may also repeat temporally. Further, to fulfil such criteria, the availability of exposures becomes an important factor. Closeness to a major intrabasinal fault, which might have remained active for a considerable period of time, becomes important in favour of seismic shocks when the role of all other agents have been refuted by the detailed analysis of observable characteristics of the host sedimentary facies along with the facies that occur just above and below.

The studied SSDS in glacio-marine deposits do not show any convincing evidence in favour of endogenic triggering agents like strong wave and tidal action, rapid sediment loading, mass-flow related shear stress, subaqueous slides and water or gas seepage. Evidences in favour of storm sedimentation are common in the studied succession, but the heteroliths that are involved in soft sediment deformations are low energy tidal deposits. Hence, the role of cyclic stresses exerted by storm waves to develop liquefaction in water saturated sediments cannot be considered as the primary cause of liquefaction. Moreover, the deformation structures occur in different stratigraphic horizons and are attributed to multiple events, which stand against the triggering for liquefaction by meteorite impact. However, in case of the muddy siltstone dykes emplaced within reverse graded conglomerate, liquefaction and fluidization may be a product strong shear stress at the base of reverse graded conglomerate or due to passing seismic waves as well. The lateral extent of the stratigraphic horizons hosting soft-sediment deformation structures could not be studied because of the unavailability of exposure outside the Dudhi Nala valley. However, episodic occurrence, closeness to a major intrabasinal fault, development close to sediment–water interface, flowage along the tilt towards the fault, confinement within undeformed beds, and close similarity of the graben-like structure that is formed during recent earthquakes are consistent with seismic triggering for liquefaction and development of the studied soft-sediment deformation structures. Moreover, absence of close association of sedimentary attributes related to other eligible triggering agents lends strong support in favour of seismic triggering. This interpretation also receives support from the revealed sequel of climatic amelioration, glacial retreat, shallow marine sedimentation, glacio-isostatic rebound and related syn-sedimentary faulting and development of SSDS.

Shanmugam (2016) raised a serious question about the status of the term ‘seismite’. According to him (Shanmugam 2016, page 321), an earthquake implies a triggering mechanism and not a flow behaviour of a depositional process, which is required for a genetic term and we should not carry the ‘genetic’ term ‘seismite’ further. His suggestion is that the term seismite (Seilacher 1969) should be considered obsolete. However, while it is true that no one has considered an earthquake as a process or mechanism for the origin of SSDS (studies on seismites referred in Shanmugam 2016, 2017), at the same time, a large number of scientists working on such structures consider that an earthquake can act as a potential trigger for liquefaction and fluidization of newly deposited soft fine-grained sediments (see references cited in Shanmugam 2016, 2017 and Sedimentary Geology special issue, 2016, Vol. 344). According to Seilacher (1969), a seismite is a sedimentary rock which contains SSDS for which liquefaction was triggered by syn-sedimentary earthquake. When the earthquake is identified as a triggering agent for liquefaction and resultant soft-sediment deformation, the present authors do find enough reasons to call the studied sediments containing the deformation structures a seismite.

5. Conclusion

The unmistakable fingerprints of seismic events mostly remain masked by other syn-sedimentary deformation structures that are not directly related

to seismic activity. Results of detailed analysis of the SSDS of the studied shallow glacio-marine setting of West Bokaro Coal Basin and arguments that are generated are consistent with seismic triggering for liquefaction of water saturated sediments. Energy released from syn-sedimentary faulting related to glacio-isostatic rebound played an important role in the formation of the studied SSDS.

Acknowledgements

The authors are thankful to two anonymous reviewers, whose constructive comments helped to improve the manuscript. The authors are also thankful to Techno India University, West Bengal for their support.

References

Allen C R 1975 Geological criteria for evaluating seismicity; *AAPG Bull.* **86** 1041–1057.

Allen J R L 1977 The possible mechanics of convolute lamination in graded sand beds; *J. Geol. Soc. London* **134** 19–31.

Allen J R L 1984 *Sedimentary structures, their character and physical basis*; Elsevier, Amsterdam **2** 663p.

Allen J R L 1986 Earthquake magnitude-frequency, epicentral distance, and soft-sediment deformation in sedimentary basins; *Sedim. Geol.* **46** 67–75.

Alfaro P, Delgado J, Estevez A, Molina J M, Moretti M and Soria J M 2002 Liquefaction and fluidization structures in Messinian storm deposits (Bajo Segur Basin, Betic Cordillera, southern Spain); *Int. J. Earth Sci. (Geologische Rundschau)* **91** 505–513.

Alvarez W, Staley E, O'Connor D and Chan M 1998 Syn-sedimentary deformation in the Jurassic of south eastern Utah – A case of impact shaking?; *Geology* **26** 579–582.

Bhattacharya H N, Mukhopadhyay G and Bose P K 1989 Hummocky cross-stratification and its hydraulic and climatic implications in Talchir Formation, Dudhi Nala, Hazaribagh, Bihar; *J. Geol. Soc. India* **34** 398–404.

Bhattacharya H N and Bandyopadhyay S 1998 Seismites in a Proterozoic tidal sequence, Singhbhum, Bihar, India; *Sedim. Geol.* **119** 239–252.

Bhattacharya H N, Chakraborty A and Bhattacharya B 2005 Significance of transition between Talchir Formation and Karharbari Formation in lower Gondwana Basin evolution – A study in west Bokaro Coal Basin, Jharkhand, India; *J. Earth Syst. Sci.* **114** 275–286.

Bose P K, Mukhopadhyay G and Bhattacharya H N 1992 Glaciogenic coarse clastics in a Permo-Carboniferous bedrock trough in India: A sedimentary model; *Sedim. Geol.* **76** 79–97.

Campbell K A, Nesbitt E A and Bourgeois J 2006 Signatures of storms, oceanic floods and forearc tectonism in marine shelf strata of the Quinault Formation (Pliocene), Washington, USA; *Sedimentology* **53** 945–969.

Chakraborty A 1977 Upward flow and convolute lamination; *Senckenbergiana Marit.* **9** 285–305.

Chen J, Chough S K, Chun S S and Han Z 2009 Limestone pseudoconglomerates in the Late Cambrian Gushan and Chaomidian Formations (Shandong Province, China): Soft sediment deformation induced by storm-wave loading; *Sedimentology* **56** 1174–1195.

Chiarella D, Moretti M, Longhitano S G and Muto F 2016 Deformed cross stratified deposits in the Early Pleistocene tidally-dominated Catanzaro strait fill succession, Calabrian Arc (southern Italy): Triggering mechanisms and environmental significance; *Sedim. Geol.* **344** 277–289.

Davies S J and Gibling M R 2003 Architecture of coastal and alluvial deposits in an extensional basin: The Carboniferous Joggins Formation of eastern Canada; *Sedimentology* **50** 415–439.

Ghosh S K 1993 *Structural Geology: Fundamentals and Modern Developments*; Pergamon, Oxford.

Greb S F and Archer A W 2007 Soft-sediment deformation produced by tides in a meizoseismic area, Turnagain Arm, Alaska; *Geology* **35** 435–438.

Hilbert-Wolf H L, Roberts E M and Simpson E L 2016 New sedimentary structures in seismites from SW Tanzania: Evaluating gas- *vs.* water-escape mechanisms of soft deformation; *Sedim. Geol.* **344** 253–262.

Jiang J, Zhong N, Li Y, Xu H, Yang H and Peng X 2016 Soft-sediment deformation structures in the Lixian lacustrine sediments, Eastern Tibetan Plateau and implications for postglacial seismic activity; *Sedim. Geol.* **344** 123–134.

Lowe D R 1975 Water escape structures in coarse grained sediments; *Sedimentology* **22** 157–204.

Lunina O V and Gladkov A S 2016 Soft-sediment deformation structures induced by strong earthquakes in southern Siberia and their paleoseismic significance; *Sedim. Geol.* **344** 5–19.

Massari F, Guibaudo G, D'Alessandro T and Davaud E J 2001 Water-upwelling pipes and soft-sediment deformation structures in lower Pleistocene calcarenites (Salento, southern Italy); *GSA Bull.* **113** 545–560.

Mastalerz K and Wojewoda J 1993 Alluvial-fan sedimentation along an active strike–slip fault: Plio-Pleistocene Pre-Kaczawa fan, SW Poland; *Int. Assoc. Sedim. Spec. Publ.* **17** 293–304.

Moretti M, Alfaro P, Caselles O and Canas J A 1999 Modelling seismites with a digital shaking table; *Tectonophys.* **304** 369–383.

Moretti M and Sabato L 2007 Recognition of trigger mechanisms for soft-sediment deformation in the Pleistocene lacustrine deposits of the Sant'Arcangelo Basin (southern Italy): Seismic shock *vs.* overloading; *Sedim. Geol.* **196** 31–45.

Mukhopadhyay G and Bhattacharya H N 1994 Facies analysis of Talchir sediments (Permo-carboniferous), Dudhi Nala, Bihar, India – Glaciomarine Model, 9th International Gondwana Symposium, Hyderabad, India, vol. 2, Oxford and IBH Publishing Co., New Delhi, pp. 737–753.

Mukhopadhyay G, Mukhopadhyay S K, Roychowdhury M and Pauri P K 2010 Stratigraphic correlation between different Gondwana basins of India; *J. Geol. Soc. India* **76** 251–256.

Nagtegaal P J C 1963 Convolute lamination, metadepositional ruptures and slumping in an exposure near Pobla de Segur (Spain); *Geologie en Mijnbouw* **42** 363–374.

Onorato M R, Perucca L, Coronato A, Rabassa J and Lopez R 2016 Seismically-induced soft-sediment deformation structures associated with the Magallanes-Fagnano Fault System (Isa Grande de Tierra del Fuego, Argentina); *Sedim. Geol.* **344** 135–144.

Owen G 1996 Experimental soft-sediment deformation: Structures formed by the liquefaction of unconsolidated sands and some ancient examples; *Sedimentology* **43** 279–293.

Owen G and Moretti M 2008 Determining the origin of soft-sediment deformation structures: A case study from Upper Carboniferous delta deposits in south-west Wales; *Terra Nova* **20** 237–245.

Owen G and Moretti M 2011 Identifying triggers for liquefaction-induced soft-sediment deformation in sands; *Sedim. Geol.* **235** 141–147.

Postma G 1983 Water escape structures in the context of a depositional model of a mass flow dominated conglomeratic fan-delta (Abrioja Formation, Pliocene, Almeria Basin, Spain); *Sedimentology* **30** 91–103.

Sarkar S, Choudhuri A, Banerjee S, van Loon A J and Bose P K 2014 Seismic and non-seismic soft-sediment deformation structures in the Proterozoic Bhander Limestone, central India; *Geologos* **20(2)** 89–103.

Seilacher A 1969 Fault-graded beds interpreted as seismites; *Sedimentology* **13** 155–159.

Seth A, Sarkar S and Bose P K 1990 Syn-sedimentary seismic activity in an immature passive margin basin (Lower Member of the Katrol Formation, Upper Jurassic, Kutch, India); *Sedim. Geol.* **68** 279–291.

Sengupta S, Chakraborty A and Bhattacharya H N 1999 Fossil Polyplacophora (Mollusca) from Upper Talchir sediments of Dudhi Nala, Hazaribagh, Bihar; *J. Geol. Soc. India* **54** 523–527.

Shanmugam G 2016 The seismite problem; *J. Palaeogeogr.* **5(4)** 318–362.

Shanmugam G 2017 Global case studies of soft-sediment deformation structures (SSDS): Definitions, classifications, advances, origins, and problems; *J. Palaeogeogr.* **6(4)** 251–320.

Sims J D 1973 Earthquake-induced structures in sediments in Van Norman Lake, San Fernando, California; *Science* **182** 161–163.

Sims J D 1975 Determining earthquake recurrence intervals from deformational structures in young lacustrine sediments; *Tectonophys.* **29** 141–152.

Su D C and Sun A P 2012 Typical earthquake-induced soft-sediment deformation structures in the Mesoproterozoic Wumishan Formation, Yongding River Valley, Beijing, China and interpreted earthquake frequency; *J. Palaeogeogr.* **1** 71–89.

Snyder M E and Waldron J W F 2016 Unusual soft-sediment deformation structures in the Maritimes Basin, Canada: Possible seismic origin; *Sedim. Geol.* **344** 145–159.

Ten Haaf E 1956 The significance of convolute lamination; *Geology Mijnbouw* **18** 188–194.

Toro B and Pratt B R 2016 Sedimentary record of seismic events in the Eocene Gran River Formation and its implications for regional tectonics on lake evolution (Bridger Basin, Wyoming); *Sedim. Geol.* **344** 175–204.

Van Loon A J 2009 Soft-sediment deformation structures in siliciclastic sediments: An overview; *Geologos* **15** 3–55.

Zhang C, Wu Z, Gao L, Wang W, Tian Y and Ma C 2007 Earthquake-induced soft-sediment deformation structures in the Mesoproterozoic Wumishan Formation, North China, and their geologic implications; *Sci. China, Earth Sci.* **50** 350–358.

Zheng L, Jiang Z, Liu H, Kong X, Li H and Jiang X 2015 Core evidence of paleoseismic events in Paleogene deposits of the Shulu Sag in the Bohai Bay Basin, east China, and their petroleum geologic significance; *Sedim. Geol.* **328** 33–54.

Corresponding editor: Santanu Banerjee